J Petrol Explor Prod Technol (2017) 7:125–146
DOI 10.1007/s13202-016-0255-5

ORIGINAL PAPER - PRODUCTION ENGINEERING

Field-scale investigation of different miscible CO_2-injection modes to improve oil recovery in a clastic highly heterogeneous reservoir

Ahmed Khalil Jaber[1] · **Mariyamni B. Awang**[2]

Received: 19 January 2016 / Accepted: 22 May 2016 / Published online: 11 June 2016

Abstract Carbon dioxide flooding is considered one of the most commonly used miscible gas injections to improve oil recovery, and its applicability has grown significantly due to its availability, greenhouse effect and easy achievement of miscibility relative to other gases. Therefore, miscible CO_2-injection is considered one of the most feasible methods worldwide. For long-term strategies in Iraq and the Middle East, most oilfields will need to improve oil recovery as oil reserves are falling. This paper presents a study of the effect of various CO_2-injection modes on miscible flood performance of the highly heterogeneous clastic reservoir. An integrated field-scale reservoir simulation model of miscible flooding is accomplished for this purpose. The compositional simulator, Eclipse compositional, has been used to investigate the feasibility of applying different miscible CO_2-injection modes. The process of the CO_2-injection was optimized to start in January 2056 as an improved oil recovery method after natural depletion and waterflooding processes have been performed, and it will continue to January 2072. The minimum miscibility pressure was determined using empirical correlations as a function of reservoir crude oil composition and its properties. Four miscible CO_2-injection modes were undertaken to investigate the reservoir performance. These modes were, namely the continuous CO_2-injection (CCO_2), water-alternating-CO_2-injection (CO_2-WAG), hybrid CO_2-WAG injection, and simultaneous water and CO_2-injection (CO_2-SWAG) processes. All injection modes were analyzed in respect to the net present value (NPV) and net present value index (NPVI) calculations to confirm the more feasible CO_2 development strategy. The results indicated that the application of CO_2-SWAG injection mode of 2:1 SWAG ratio attained the highest oil recovery, NPV and NPVI, among the other modes. The achieved incremental oil recovery by this process was 9.174 %, that is 189 MM STB of the oil produced higher than the waterflooding case, 1.113 % (23 MMSTB of oil) in comparison with the CCO_2-flooding case, 1.176 % (24.3 MMSTB of oil) in comparison with the hybrid CO_2-WAG case and almost 0.987 % (204 MMSTB of oil) when compared with the CO_2-WAG case. The results indicated that the application of CO_2-WAG injection mode of 1.5:1 WAG ratio attained the highest oil recovery after the SWAG process.

Keywords CO_2-injection · Clastic heterogeneous reservoir · Field-scale analysis

List of symbols

NPV	Net present value, USD
NPVI	Net present value index
CNPV	Cumulative net present value, USD
MCO	Maximum capital outlay, minimum value on the cumulative NPV curve, USD
FOE	Field recovery factor, fraction
FOPT	Field oil production total, STB
FOPR	Field oil production rate, STB/day
FWCT	Field watercut total, fraction
FPR	Field pressure, psia
CAPEX	Capital expenditure, USD
OPEX	Operational expenditure, USD

✉ Ahmed Khalil Jaber
ahmedkhalil1974@yahoo.com

[1] Iraqi Ministry of Oil & Universiti Teknologi PETRONAS, 31750 Tronoh, Perak, Malaysia

[2] Universiti Teknologi PETRONAS, 31750 Tronoh, Perak, Malaysia

NCF	Net cash flow, USD
t	Future time, year
T	Cumulative investment (or production) period
i	Interest rate, fraction
Q_w	Water injection rate, STB/day
Q_{CO_2}	CO_2-injection rate, Scf/day
B_{CO_2}	CO_2 formation volume factor, rbbl/Scf
B_w	Water formation volume factor, rbbl/STB
$WACO_{2ratio}$	Water-alternating-CO_2 ratio
N_{ca}	Capillary number
υ	Velocity of the displacing phase
μ	Viscosity of the displacing phase
σ	Interfacial tension between oil and water
θ	Contact angle between oil–water interface and the rock surface
P_c	Capillary pressure, psi
Sw	Water saturation
Sw_n	Normalized water saturation
Krw_n	Normalized water relative permeability
Kro_n	Normalized oil relative permeability
nw	Water exponent parameter
no	Oil exponent parameter

Introduction

CO_2-flooding appeared in the 1930s and had great development in the 1970s (Hao et al. 2004). With over 40 years of production practice, CO_2-flooding has become a leading EOR technique for light and medium oils (Reid and David 1997). CO_2-flooding is beneficial for both the environment and the petroleum industry by injecting the harmful CO_2 to increase oil recovery. This reduces greenhouse gas emissions by sequestration of CO_2 in the reservoir, thus reducing heat trapped in the atmosphere. CO_2-injection has been proved as a successful technology worldwide, with less minimum miscibility pressure than nitrogen and hydrocarbon gases. The studied reservoir was the Nahr Umr reservoir which is considered one of the most important producing reservoirs in the south of Iraq. This reservoir as with many of the southern Iraqi fields needs to apply improved oil recovery methods (IOR) in the nearest future to extract more oil and increase oil recovery. It is very necessary to screen, investigate and optimize the proper IOR method. IOR technology using CO_2-injection has been proven to be more profitable during recent years. CO_2-injection has a great potential of enhancing and increasing oil recovery. However, it does not recover all the oil, regardless of whether the reservoir has been previously flooded with water. Typically, recovery addition with miscible CO_2 displacement is around 10–20 %, by injecting an equivalent of 80 % HCPV with CO_2 (Marylena 2005).

The heterogeneity index for the Nahr Umr reservoir in the Subba oilfield was determined based on Lorenz coefficient calculations. This was based on the flow capacity distribution to measure the contrast in the permeability relative to the homogeneous case (Ganesh and Satter 1994). The average Lorenz coefficient value for different core samples of the Nahr Umr reservoir was found equal to 0.814, which indicates that this reservoir is a highly heterogeneous reservoir. The Subba oilfield has a short history, as the experimental period during the 1990s. The production of the field did not last due to some technical issues at that time. The reservoir heterogeneity measurements vary depending on the scale of the measurement. Webber and Van Geuns (1990) discovered that the geological heterogeneity also varies depending on the scale of the measurement. The reservoir heterogeneity has a significant impact on fluid flow. It is, therefore, crucial to investigate the CO_2-flooding behavior with the field-scale heterogeneity model. This model is able to incorporate all the reservoir heterogeneity. Most of the CO_2 studies have been investigated with small-scale experimental core measurements. It is difficult to incorporate the reservoir heterogeneity into the small-scale measurements (Webber and Van Geuns 1990). There have been few works on CO_2-flooding in small-scale heterogeneity carried out (Bennion and Bachu 2006). One of the significant features of the current study is the effect of the full-field-scale heterogeneity on oil recovery and sweep efficiency across a heterogeneous model during CO_2-flooding.

Due to the reservoir's heterogeneity, the optimal locations and number of infill wells were optimized based on sweet spots determined by dynamic opportunity index analyses (Al-Khazraji and Shuker 2015b). There were 50 infill wells and, accordingly, 21 injectors were decided to be involved in the development scenarios. The waterflooding process has been optimized to start up in January 2028 and will continue till January 2056 with 3000 bbl/day as the water injection rate for each well. The CO_2-injection is proposed to commence in January 2056 as an IOR method after the waterflooding process and will be tested till January 2072. In this study, four production strategies with different sensitivities under miscible CO_2 were examined to optimize the best long-term miscible flooding strategy for the reservoir. These strategies include CCO_2-injection with different slug sizes, CO_2-WAG with different half-cycle rates, CO_2-SWAG and hybrid CO_2-WAG injection with different slug sizes. The compositional flow simulation model, Eclipse compositional, was used to construct the flow simulation runs. Eclipse compositional allowed the researcher to model a multicomponent hydrocarbon flow in order to get a detailed description of the

phase behavior and compositional changes, and it used a cubic equation of state (EOS). The obtained results were analyzed depending on the NPV and NPVI analysis of the produced oil that were conducted for each case.

Background

The CO_2-flooding process can be classified as miscible and immiscible. In the immiscible flooding process, the relatively high reservoir pressure results in the CO_2 dissolution, oil viscosity reduction, lowering of interfacial tension, oil swelling and dissolved gas drive. In the miscible flooding mechanism, the process involves the generation of the miscibility at the minimum miscible pressure between the CO_2 and reservoir oil, lowering the interfacial tension between the oil and CO_2, and swelling of the oil due to the transferring of the CO_2 into the oil, then, lowering the oil viscosity and density, and finally the increasing oil recovery factor. The miscibility between the CO_2 and crude oil was achieved through the multiple contact miscibility process. CO_2 was first condensed into the crude oil (transferring of CO_2 to the oil), making oil lighter. The lighter components of the oil vaporized or were extracted by the reminder of the CO_2, making the CO_2 denser with a higher viscosity. The formed CO_2 is called the rich phase; as the mass transfer continued between the CO_2 and oil, the formed CO_2 became more like oil in terms of fluid properties. The relative permeability of the gas (displacing phase) was reduced, and the mobility ratio was reduced. The capillary number increased, microscopic displacement efficiency increased, and then the recovery factor was increased. The capillary number was defined by the following equation.

$$N_{ca} = \frac{\text{Viscouse Forces}}{\text{Capillary Forces}} = \frac{\upsilon\mu}{\sigma\cos\theta} \quad (1)$$

where υ and μ are the velocity and the viscosity of the displacing phase, respectively, σ is the interfacial tension between the oil and water and θ is the contact angle between the oil–water interface and the rock surface measured between the rock surface and the denser phase. This takes place because the purpose of any EOR method is to increase the capillary number that leads to a favorable mobility ratio ($M < 1.0$).

Using CO_2 as the miscible gas injection is considered one of the more successfully enhanced oil recovery methods worldwide. The major factor affecting implementing the CO_2-flooding is the economic criteria, i.e., its availability at an economical price (Mohamed et al. 2012). The net utilization ratio of CO_2 per barrel of additional oil recovered varies from field to field, but on average has been estimated at 5.5 MSCF CO_2 per additional barrel of oil in the USA EOR overview study by Broome et al. (1986) and between 4 and 6 MSCF/barrel by a more recent study by Jeschke et al. (2000). In the USA, about 20 % of the total EOR production was obtained by CO_2-flooding in 1992 (Ganesh and Satter 1994).

A comparison of EOR surveys (Rao et al. 2004; Kulkarni and Rao 2004) from 1971 to 2004 showed a significant increase in the petroleum industry trend toward miscible gas injection EOR. The miscible gas injection accounts for nearly 80 % of the gas injection EOR (Kulkarni and Rao 2004). The CO_2 share of the gas injection EOR oil increased from 39 % in 1984 to 65 % in 2004 (Rao et al. 2004; Kulkarni and Rao 2004). Generally, CO_2-injection can prolong the reservoir life for 15–20 years and may recover an additional 15–20 % of the original oil in place (Hao et al. 2004); this is mainly due to a higher microscopic displacement efficiency of the CO_2-flooding (Chen et al. 2009). However, CO_2-flooding suffers from poor macroscopic displacement efficiency in a heterogeneous reservoir due to the low viscosity of CO_2. This leads to early a CO_2 breakthrough, unstable pressure distribution, viscous fingering, channeling and bypass oil resulting in reduced oil recoveries. Therefore, the WAG technique process was proposed to improve the sweeping efficiency of injected gas, control the mobility of the gas and stabilize the displacement front since the WAG technique combines the improved microscopic displacement efficiency by gas with improved macroscopic displacement efficiency by water. The WAG flooding process was first applied in 1957 in Canada and reported in the literature by Caudle and Dyes in 1957. In recent years, the WAG process has gained an increasing interest for EOR in the USA; approximately 55 % of the total oil productions employing EOR methods are a result of gas injection methods, the majority of which are WAG processes. The literature review suggests that almost 80 % of the gas injection processes employ the WAG flooding process (Mohamed et al. 2012).

Many studies suggested that the CO_2-WAG flooding process has usually been applied as a tertiary recovery method of flooding (Christensen et al. 1998; Babadagli 2005; Hadlow 2004). In contrast, many other studies indicated that the application of the WAG process in the early stages of the reservoir life produces an outcome of higher oil recovery with less pore volume being injected (Mahnaz and Farouq 1984; Shyeh-Yung 1991; Thomas and Leiv 2002; Mohamed et al. 2012; Behrouz and Ghazanfari 2004). Kulkarni and Rao (2005) indicated in their experimental work that the secondary mode miscible corefloods demonstrated high oil recoveries. Several CO_2-flooding methods that have been used for EOR include:

1. Continuous CO_2-injection (CCO_2),
2. Injection of water and CO_2, simultaneously (CO_2-SWAG),

3. Injection of CO_2 and water, alternately (CO_2-WAG);
4. Hybrid CO_2-WAG injection process in which a large volume of gas is initially injected, followed by a number of small slugs of water and gas being injected (Christensen et al. 1998).

Research objectives

The main objective of the current study has been to investigate different modes of miscible CO_2-flooding performance in a highly heterogeneous reservoir through a full-field-scale analysis. Four modes of miscible CO_2-flooding were examined for future reservoir performance prediction. These modes included the CCO_2-injection, CO_2-WAG, simultaneous water and CO_2-injection (CO_2-SWAG) and hybrid CO_2-WAG injection techniques.

To achieve the objectives of this study, the following tasks had to be fulfilled:

1. Determining the optimum continuous CO_2-injection rate.
2. Determining the optimum injection CO_2-WAG ratio.
3. Determining the optimum CO_2-WAG half-cycle length.
4. Determining the optimum CO_2-injection rate for the CO_2-SWAG process.
5. Determining the optimum CO_2-SWAG ratio.
6. Determining the optimum CO_2 slug size for the hybrid CO_2-WAG process.

Methodology

In order to accomplish the aforementioned objectives, the following steps had to be followed:

1. Building the petrophysical study of the reservoir by employing Interactive Petrophysics (IP) software from Senergy Ltd.
2. Generating a PVT model of the reservoir by employing the Peng–Robinson cubic EOS by using Petroleum Expert PVTP software.
3. Building a 3D static geological model by employing Schlumberger Petrel software.
4. Generating a compositional simulation flow model through utilizing Eclipse compositional in order to demonstrate the effect of the miscible CO_2-flooding process for improving oil recovery.

Reservoir characterization and description

The Subba oilfield is located in the Southeast of Iraq, some110 km to the Northwest of Basra and 12 km Northwest of the Luhais oilfield. The Subba oilfield is described as a giant oilfield with bottom and edge water support. There were 14 wells drilled in this field which penetrated the Nahr Umr formation; but, only six of them were completed in the Nahr Umr reservoir.

The dimensions of the Subba oilfield are about 30 km long and 7 km wide. The Nahr Umr reservoir is considered one of the most important productive reservoirs in the Southern Iraqi fields, which comprises an important place in the stratigraphic column of the Lower Cretaceous Albian Nahr Umr. It has a double dome separated by a shallow saddle. The largest one is located in the South of the field and the smallest one in the North of the field. This field has not been developed for over the last 40 years, since it was produced in 1990 for a short experimental period from the Nahr Umr reservoir.

Static model

The purpose of the geological interpretation is to generate a robust 3D geological facies model of the Nahr Umr clastic reservoir in order to capture the lateral and vertical reservoir heterogeneity. The heterogeneity of the reservoir is dependent on the depositional environments and subsequent events (Ahmed 2010). The goal of reservoir characterization for heterogeneous formations is to establish a reservoir model based on explicitly modeling the known heterogeneities (conditioning to well observations) and using mathematical and geostatistical algorithms to systematically simulate the spatial distribution of the reservoir properties at inter-well locations. The modeled area was about 787 km^2.

The Nahr Umr formation comprises a lower Cretaceous Albian clastic unit. This unit characterized by massive clean sands, which are overlain by a mixture of shale, silt and massive clean sand interbedded with shale. The formation is composed generally of interbedded black shale with coarse- to fine-grained sandstone (Aqrawi et al. 2010). The Nahr Umr formation in the South of Iraq is interpreted to be an alluvial to lower coastal plain to a deltaic deposit with shallow marine and aolian influences (Aqrawi et al. 2010). The crest of the structure in the Subba oil field occurs at a depth of (−2403) m SSTVD. The average thickness of the reservoir is about 195 m. The average pay thickness of the reservoir is about 26 m.

The Nahr Umr reservoir in the Subba oil field has been described from core photographs and a core description of 500 meters of the reservoir in the field through seven wells. The core data and description have been integrated with a wireline log response to aid in the development of the geological model and in facies and reservoir quality predictions. There were four major facies groups were identified from the core photo description. These facies include sand fluvial, sand tidal for the reservoir, siltstone and shale for the nonreservoir. Accurate high-resolution model is critical to have a better understanding of the reservoir heterogeneity for enhanced oil recovery. The geological model of the Nahr Umr formation has been constructed by utilizing Schlumberger's Petrel software in order to incorporate all available structural, logs and facies data.

The static model was constructed based on the petrophysical interpretation results (Al-Khazraji and Shuker 2014a, b, 2015a, b), structural contour maps of the formation geological layers and data from 14 wells penetrating the reservoir. These data comprised well coordinates, formation tops, core data, log interpretation results, facies and permeability curves (Al-Khazraji and Shuker 2014b; Well logs for Nahr Umr formation—Subba oilfield 1973–1980; final well reports for Nahr Umr formation—Subba oilfield 1976–1990; final geological reports for Nahr Umr formation—Subba oilfield, 1976–1990; core measurements reports for Nahr Umr formation—Subba oilfield 1976–1980; geological study for Subba oilfield 2001). The log interpretation results included shale volume, porosity and water saturation. The petrophysical properties distribution, such as permeability, porosity and saturation, was constructed based on the facies model. The resultant 3D cellular model formed the basis for the reservoir simulation model that was used to optimize the reservoir development scenarios. The Nahr Umr reservoir has a heterogeneous permeability profile, including very high permeability for sandstone and very low permeability for shale.

Structural modeling

The model cells were defined as 200 m × 200 m in the *X*- and *Y*-directions with 36 cell layers deep. The model was constructed of 36 cell layers deep, with the layer thickness differing and ranging as follows: 2.81 m for layers (1–8), 12.28 m for layers (9–12), 3.91 for layers (13–24) and 8.52 for layers (25–36). This size of cells was efficient to capture the reservoir characteristic and the reservoir petrophysical property changes as well as to ensure that the derived geological grids could be exported into the simulation model directly, hence avoiding grid upscaling. The number of layers in the geological model was adjusted to ensure the match between the upscaled and well facies. Then, a better definition was set for discrete flow units and the boundaries that separated the flow units in the reservoir.

The total number of cells considered in the geological model was set to 101 and 196 in the *X*-direction and *Y*-direction, respectively, considering 36 cells in the Z-direction. The total number of cells in the geological model became 712656 cells.

Petrophysical modeling

The generated heterogeneous distribution for porosity and permeability was matched with core laboratory measurements. The petrophysical derived log properties, porosity, permeability and water saturation, were scaled up into the cellular model. The scale up of the well logs was an automatic process with some user settings available. When scaling up the well logs Petrel software will first find the 3D grid cells that the wells penetrate. For each grid cell, all log values that fall within the cell will be averaged according to the selected algorithm to produce one log value for that cell (Petrel Seismic-to-Simulation software manual 2013). The petrophysical properties are modeled stochastically using the sequential Gaussian simulation (SGS) method, allowing for finer-scale heterogeneity and greater control as well as prediction of the petrophysical properties in areas away from the well data points. It assumes that the data to be modeled would have a Gaussian distribution from the upscaled logs.

Original oil in place (OOIP)

The volume of oil originally in place's calculations was very important before embarking to reservoir performance prediction. The deterministic approach of the volumetric method was used in the original oil in place (OOIP) estimating for the reservoir, based on geological modeling calculations. The OOIP resulting from the geological modeling was basically consistent with that resulting from the volumetric method. The value of the initial oil formation volume factor (Boi) considered in the OOIP calculations was established from the PVT data at the initial pressure and was found to be equal to (1.18191 rbbl/STB). The estimated OOIP of the reservoir calculated from the static model was found to be equal to (1.9695 MMMSTB).

Pressure and temperature

The Nahr Umr reservoir is an understated reservoir with an initial formation pressure of 4084 psia, which is 2981 psia above its oil bubble point pressure of 1103 psia. The

reservoir temperature is considered dependent on the field measurement corrected to the datum level (2500 m SSL) which was found to be equal to 178 °F.

Boundary conditions

In this study, flow boundaries from the surrounding aquifer, bottom and edge have been considered as they have proved from well logs, well tests and production log test. The Carter–Tracy analytical aquifer model (PVT experiments report for Nahr Umr formation—Subba oilfield 1978) was adopted in the reservoir simulation flow model to represent the water influx drive mechanism. The support expected in this field was active because the water initially in place volume was found to be more than ten times the oil initially in place.

Fluid properties

The oil had a stock tank gravity of 28° API, and it was highly undersaturated at initial reservoir conditions. The estimated producing gas oil ratio is 389.4 STB/bbl (61.91 m^3/m^3) based on the laboratory PVT differential liberation experiments and EOS fluid modeling results. The oil was of good quality with zero sulfur content. The fluid properties of the reservoir are shown in Table 1. For the compositional simulation runs, the Peng–Robinson cubic equation of state was employed.

Model initialization

The initialization model specified a pressure of 4080 psi at the reference depth of 2500 m. Oil–water relative permeability and capillary pressure data were used. The average reservoir temperature was found to be equal to 178°F based on the field and laboratory measurements at 2500 m.

Table 1 Reservoir fluid properties

T, °F	178
Pb, psia	1103
ρ_o, °API	28.7
μ_O @ Pb, cp	1.6183
$_{Bo}$ @ Pb, rbbl/STB	1.189
γ_ω	1.1678
μ_w, @ Pinit, cp	0.7000
γ_g	0.6534
$_{Bw}$ @ Pinit, rbbl/STB	1.0160

Capillary pressure and relative permeability

Relative permeability is one of the most important parameters that affect the fluid flow in the simulation model. The shape of the P_c and K_r curves, as well as their endpoints, was very important to accurately model fluid flow in the reservoir. The water and oil relative permeabilities are two of the most sensitive and important reservoir parameters when evaluating any reservoir's water breakthrough and waterflood potential. The relative permeability curves control the relative mobility of the fluid phases in the reservoir. They consequently influence displacement efficiency, and, to a lesser extent, sweep efficiency. It is critical to obtain reliable and realistic relative permeabilities for input into the simulator. Similar to capillary pressure curves, care should be taken in the preparation of the relative permeability data for the simulation models in order to have a simulation model that runs efficiently and accurately. The curves should be smooth and monotonic, and end point saturations between the drainage capillary pressure, imbibition capillary pressure and relative permeability curves should be consistent. In the current study, the measured core laboratory capillary pressure and relative permeability curves were used. However, the capillary pressure was scaled on the basis of the Leverett J-function (Leverett 1941) for the permeability, porosity and interfacial tension.

Air–brine restored state capillary pressure measurements were conducted for ten reservoir core plugs. These experiments' data were divided into four groups based on the permeability and connate water saturation of the core plugs. The arithmetic average of the connate water saturation values was assigned to each group. The water saturation values were normalized, and the determination of the corresponding dimensionless Leverett J-function (Ahmed 2005) was used to convert the capillary pressure curves for each group into a universal curve. Four J-function equations were generated for all the rock types. The water saturation values were de-normalized, and the determination of the corresponding Leverett J-functions was generated as a function of the normalized water saturation (Sw_n) by selecting arbitrary values of Sw_n. The resulting Leverett J-functions have been plotted versus the corresponding water saturation. The best-fit line for each rock type was finally generated. The resulting capillary pressure (P_c) equation for each rock type was as follows:

$$P_C = 120.12 * \left(0.0724 * Sw^{-0.951}\right)\sqrt{\frac{764.25}{0.3}} \quad (2)$$

$$P_C = 120.12 * \left(0.1302 * Sw^{-0.923}\right)\sqrt{\frac{245}{0.11}} \quad (3)$$

$$P_C = 120.12 * \left(0.114 * Sw^{-1.59}\right)\sqrt{\frac{130}{0.05}} \quad (4)$$

$$P_C = 120.12 * \left(0.0951 * Sw^{-3.31}\right)\sqrt{\frac{30.7}{0.015}} \quad (5)$$

There were twelve relative datasets of permeability measurements conducted on twelve core samples harvested from 5 wells in the reservoir. The experiments were conducted under ambient conditions using the unsteady state method, with oil and brine as the test fluids. Corey's correlations (Corey 1954) were used to make gas–oil and water–oil relative permeability curves for the four different rock types in the model and correlate the laboratory data as follows:

$$krw_n = Sw_n^{nw} \quad (6)$$

$$kro_n = (1 - Sw_n)^{no} \quad (7)$$

The weighted average normalization respect to the capacity (kh) was determined for the oil and water relative permeability values as a function of the normalized water saturation by selecting arbitrary values of the normalized water saturation. The corresponding average Corey exponent parameters that matched the average normalized relative permeability curves were then adjusted. The de-normalization process was finally assigned to the different rock types based on the existing connate water saturation (Swc) for each rock type. The values of the residual oil saturations (Sor) and end points relative permeabilities ($krw_{@Sor}$, and $kro_{@Swc}$) for each rock type were determined through the weighted average in respect to the (porosity *x* thickness) and the capacity (kh) for the residual oil saturation and end point relative permeability, respectively. The laboratory measurements of the relative permeability curves suggested that the reservoir rocks were almost behaving as oil wet as supported by the crossover point in the data which mostly occurring at saturations less

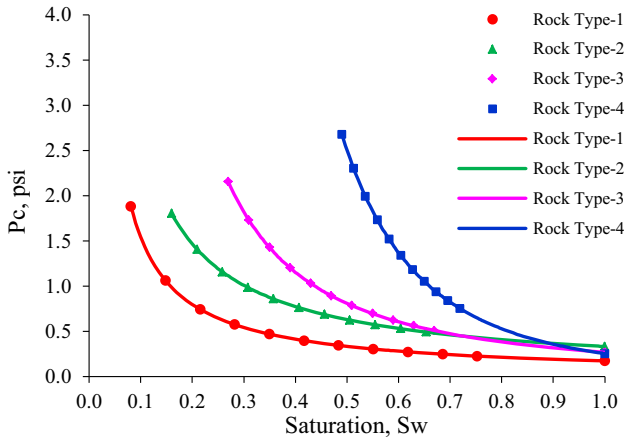

Fig. 1 Capillary pressure curves for the Nahr Umr reservoir—Subba oilfield

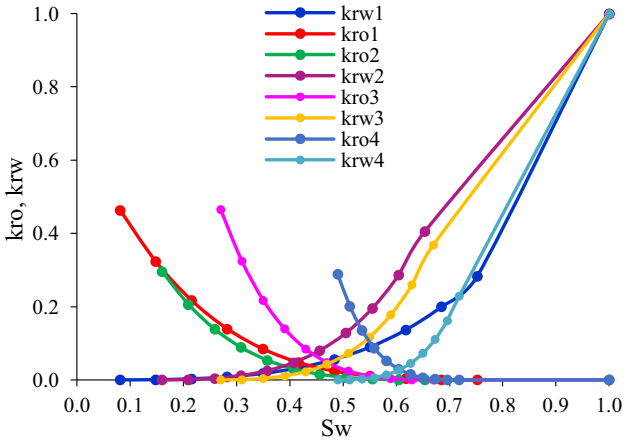

Fig. 2 Relative permeability curves for four rock types in the Nahr Umr reservoir (water–oil system)

than (50 %). Figures 1 and 2 show the capillary pressure and relative permeability curves for the four rock types.

For the gas–oil relative permeability, there were 14 sets of relative permeability data measurements conducted on 14 core samples taken from four wells in the reservoir. The same approach followed in the oil–water relative permeability is shown previously was used to create the gas–oil relative permeabilities. Figure 3 shows the oil–gas relative permeability curves for the two active rock types that were used in the simulation model. In the simulation model, gas and oil were considered as the miscible components that mean that there was no capillary pressure between the oil and gas.

PVT model

The PVT model was accomplished by employing IPM-PVTP fluid thermodynamic software from Petroleum Experts Ltd. The Podbielniak compositional analyses were conducted for a bottomhole fluid sample of the reservoir. The fluid properties were calibrated with the EOS compositional model to match the measured laboratory data. Ten components of the reservoir fluid sample till C6+ were used to generate the cubic Peng–Robinson EOS as shown in Table 2. The model adjusted the component properties to match the observed fluid properties. The field's production separator conditions were incorporated in the PVT model calculations, as indicated in Table 3. Five-stage tests were performed on the fluid sample including the stock tank, the liberated GOR and gas specific gravity at each separation step. In the current study, the single stream mode was utilized to match the laboratory data which included the adjusting properties, i.e., the component properties of one stream were changed to match its laboratory data. The component compositions

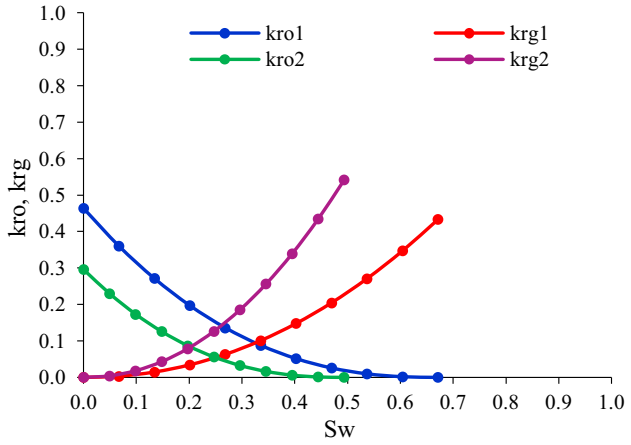

Fig. 3 Relative permeability curves for two rock types in the Nahr Umr reservoir (gas–oil system)

Table 2 Composition of the injected gas

Component	Z_i (Mole-frac)
N_2	0.001
CO_2	0.998
C_1	0.001

Table 3 Separator stages for the Nahr Umr reservoir

Separator Stage	1	2	3	4	Stock tank
Pressure (psig)	600	255	27	12	0
Temp. (°C)	60	60	60	60	60

were kept with no change. The following EOS parameters were adjusted to achieve the match of the global ΩA and ΩB (the same value of each was used for all the components), the critical temperature (T_c) and critical pressure (P_c) for the pseudo-components and the nonhydrocarbon components (N_2, CO_2). The T_c and P_c of the fluid components were selected as the regression parameters to be tuned in order to obtain the laboratory data matched for all the fluid properties except the fluid viscosity, which was predicted separately by using the Lohrenz, Bray and Clark model (Lohrenz et al. 1964). This correlation used the composition, specific gravity and, more importantly, critical volume (V_c), which was the dominated parameter as it was the most significant input parameter for the model.

It was very unlikely that a satisfactory match to the observed properties would be obtained before applying a multivariable nonlinear regression process. Therefore, a nonlinear regression analysis was carried out to get the match between the laboratory experimental results and the modeled fluid properties. The following experimental results were used as match parameters:

1. Bubble point pressure from the differential liberation dataset.
2. Fluid density at the bubble point pressure from the differential liberation dataset.
3. Oil formation volume factor (B_o) versus pressure from the differential liberation dataset.
4. Oil density versus pressure from the differential liberation dataset.
5. Solution of gas oil ratio (R_s) versus pressure from the differential liberation dataset.
6. Stock tank oil density for the differential liberation dataset.

While tuning the EOS, it is important to recognize that the purpose of doing so is to provide a tool which is capable of predicting fluid behavior away from the experimental conditions. The combination of the EOS having many parameters to adjust, and the availability of powerful multivariable regression algorithms, means that there is a danger that the EOS can be forced to match the tuning data to such a degree that it cannot predict the behavior under other conditions accurately. In order to avoid this, the regression was limited to those parameters which were known with least certainty and only moderate changes were allowed. In the current study, no components splitting was required to achieve the EOS parameters match because the ten-component PR-EOS description reflected a good match to the PVT data. The matched results are presented in Figs. 4, 5, 6, 7 and 8.

Minimum miscibility pressure (MMP)

The minimum miscibility pressure (MMP) is the minimum pressure for a specific temperature at which miscibility can occur independently of the overall composition (El-Maghraby et al. 2011). For the miscible CO_2-injection project, the reservoir pressure must be maintained at the minimum miscibility pressure or higher. The MMP is reported to be a function of temperature and fluid compositions. Several methods for determination of the MMP have been proposed: slim tube experiments, calculations with EOS and correlations. There was no availability of slim tube experiment results or the experiments required to conduct the EOS analysis for the Nahr Umr reservoir. Therefore, it depended on the available correlations to determine the minimum miscibility pressure. Several empirical correlations were tested, including Glaso (1985), Yellig and Metcalfe (1980), Yuan and Johns (2004), Cronquist (1978) and Alstone (1985); the results are shown in Table 4. The MMP calculated by the Glaso (1985) method was found equal to 2425 psia. This was considered in the current work because, the average molecular weights

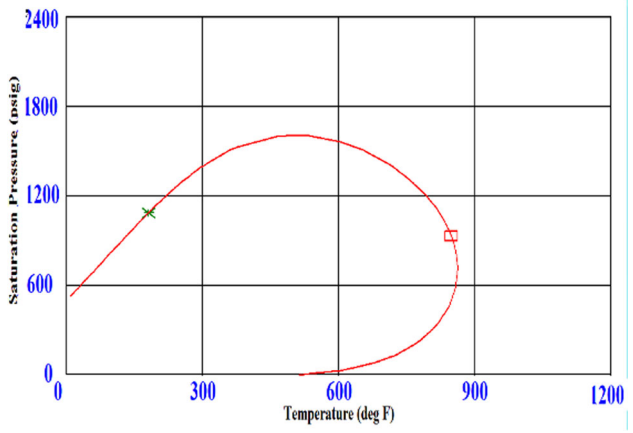

Fig. 4 Bubble point pressure match on phase envelope after regression

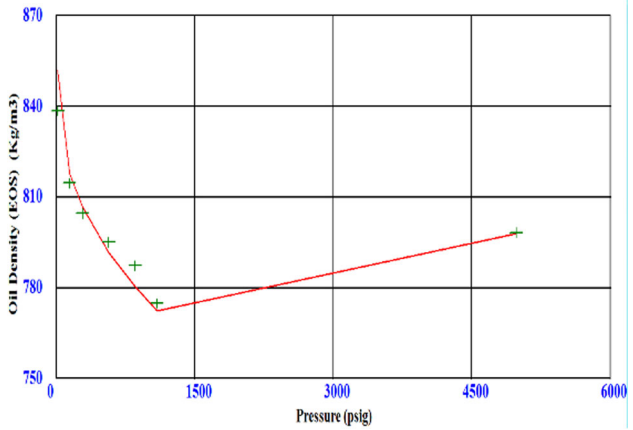

Fig. 5 Differential liberation oil density match after regression

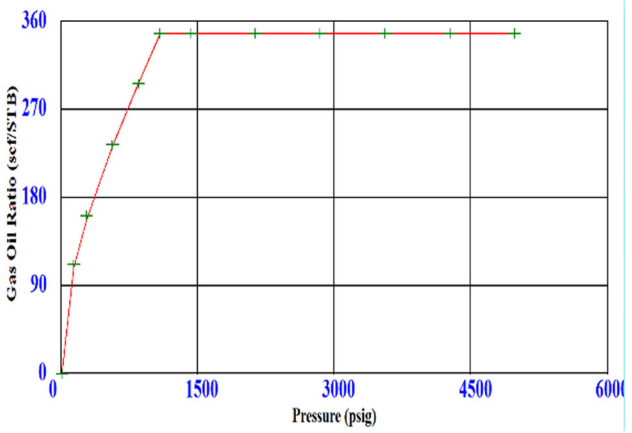

Fig. 6 Differential liberation gas oil ratio match after regression

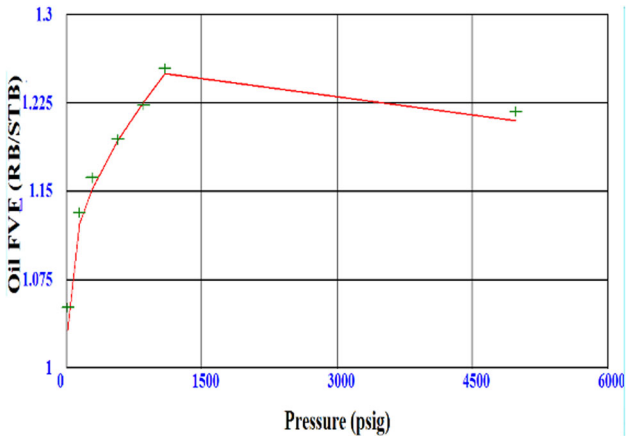

Fig. 7 Differential liberation oil formation volume factor match after regression

of the fluid samples used the in Glaso correlation, almost near the molecular weight of the Nahr Umr fluid and it gave an average value as well.

Economic calculations

To prove the success of any project, economic calculations have to be performed to examine the project feasibility. The technical success of the project alone sometimes is not enough to give the final decision of the project's success as many projects have proved to be technical successes but not economical ones.

To build a sound business decision, it requires economical criteria for measuring the value of the proposed investments and financial opportunities (Ganesh and Satter 1994). The objectives of carrying out an economical analysis were to select the best development strategy for the field based on the minimum costs and high profit. The net present value is considered as one of the most economical criteria that are widely used to include the time value of money and is considered as a measure of profit. It is defined as the aggregate of all project cash flows for a specified time period, discounted back to a common point in time. In this study, a fixed discount rate of 10 % per annum was considered. NPV was determined by calculating the present worth of all the future net cash flows and summing them up. The future cash flow includes all sales revenue of the produced oil and gas minus the costs of water handling, water reinjection, capital expenditures (CAPEX), operational expenditures (OPEX) and transportation cost of oil discounted at a 10 % annual rate. The operation cost escalation was considered to be 1.5 % (Ghomian 2008). This included the lifting cost, water handling, reinjection and recycling costs. The inflation rate of the oil prices was considered in this study as it causes prices to rise over time. Oil prices had a big fall in mid-2014 to US$ 44 and stopped falling at the end of the same

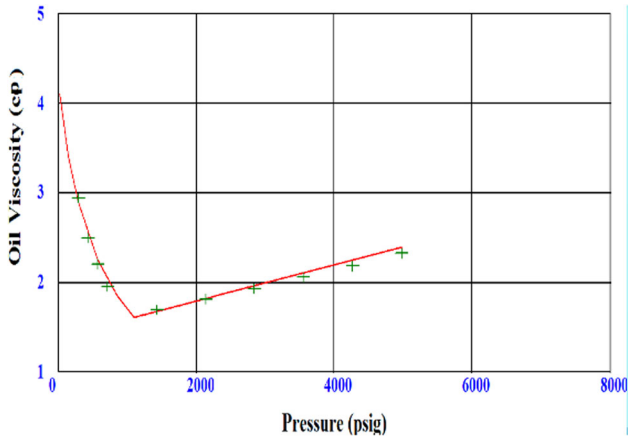

Fig. 8 Differential liberation oil viscosity match after regression

Table 4 Minimum Miscibility Pressure Calculations

Correlation	Minimum miscibility pressure (psia)
Glaso (1985)	2425
Yellig and Metcalfe (1980)	2221
Yuan and Johns (2004)	2659
Cronquist (1978)	2894
Alstone (1985)	3269

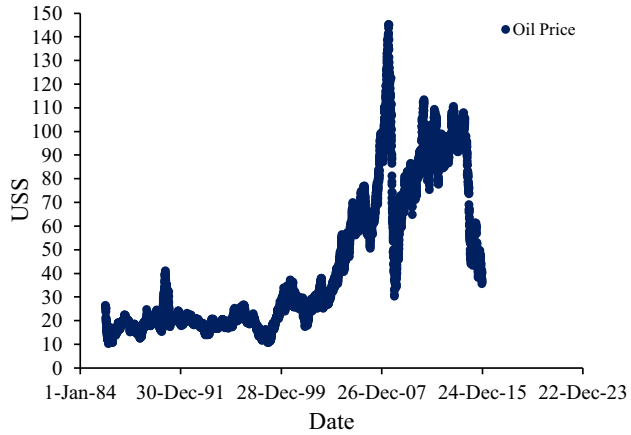

Fig. 9 Statistic historic of oil prices

year and then fell again to US$ 36 at the end of 2015 as presented in Fig. 9. The variability of oil prices makes it difficult to expect the exact trend of the inflation rate. As oil prices move up or down, inflation follows in the same direction. The reason why this happens is that oil is a major input in the economy and it is used in critical activities, such as fueling transportation and heating homes. If the input costs rise, so should the cost of the end products. In this study, a ratio of a 5 % inflation rate per annum was assumed to be more reasonable to keep pace with the oil market. Gas prices were assumed to be constant over the project life.

The cost of existing producing wells was considered already incurred during the natural depletion phase of the field. The royalty and taxes were neglected in this analysis as the oil fields are owned and developed by the Iraqi government. The NPV was computed using the following formula (Ganesh and Satter 1994; Nwaozo 2006):

$$\mathrm{NPV} = \sum_{t=1}^{T} \frac{\mathrm{NCF_t}}{(1+i)^{\mathrm{t}}} \tag{8}$$

$$\begin{aligned} \mathrm{NCF(t)} &= \mathrm{Revenue} - \mathrm{CAPEX} - \mathrm{OPEX} \\ &- \mathrm{Water\ handling\ and\ reinjection} \\ &- \mathrm{Transpotation\ cost} - \mathrm{CO_2price} \\ &- \mathrm{CO_2Recycle\ cost} \end{aligned} \tag{9}$$

In a comparison of the NPV profile for different injection modes, it has been hard to present a rigorous decision among them as the NPV profile was changing throughout the production period. Therefore, it's another economic criterion was introduced to assist making a sound decision; this economic criterion is called the net present value index (NPVI). The NPVI was very useful to measure the investment and profit efficiency, and it was calculated using the following equation:

$$\mathrm{NPVI} = \frac{\mathrm{CNPV}}{\mathrm{MCO}} \tag{10}$$

In order to perform the NPV and NPVI calculations, the economical parameters shown in Table 5 were used in this study (Al-Khatteeb 2013; Bailey et al. 2000; Al-Mudhafar 2013). The capital expenditures included the cost of production facilities, water injection facilities, injection well drilling, completion, cementing, perforation and acidizing services. The water handling and reinjection processes included: pumping, electricity, treatment equipment, storage equipment, piping and maintenance.

Reliability of the reservoir simulation model

It is essential to conduct miscible flooding for highly a heterogeneous reservoir on a full-field scale. Webber and Van Geuns (1990) discovered that the geological heterogeneity varies depending on the scale of the measurement. In essence, at a given scale, such as the microscopic level, confuse within the individual reservoir unit, cross-bedding and lamination can be identified and thus have significant an impact on fluid flow. Three wells have been reported to be produced from the reservoir over a short period. The cumulative oil production of these wells was: 1205 STB in

Table 5 Economic parameters for the Nahr Umr reservoir

Interest rate (%)	10
Oil price ($/STB)	50
Net gas price ($/MSCF)	3.5
Water handling ($/STB)	0.373
Water re-injection ($/STB)	0.559
OPEX ($/STB)	1.5
Well capex (MM$)	5
Average crude oil transportation cost ($/STB)	2.7
Water injection facilities (MM$)	17
Production facilities (MM$)	100
CO_2 capturing and compression ($/MScf)	0.85
CO_2 transportation ($/MScf)	0.25
CO_2 recycle ($/MScf)	0.35
Capex of CO_2 separation, treatment and re-injection (MM$)	22

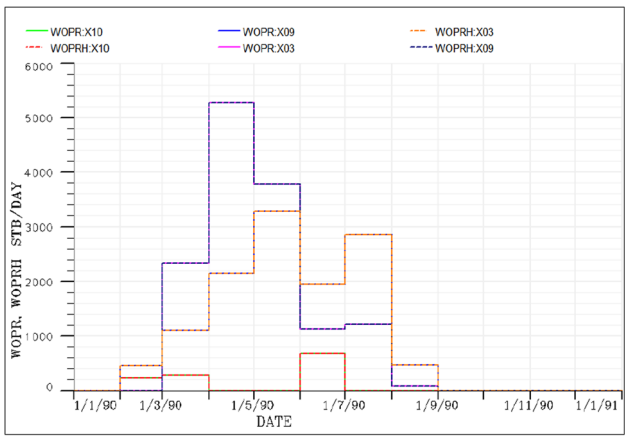

Fig. 10 History match for well oil productions

3 months, 12269 STB in 6 months and 13816 STB in 6 months. The reliability of the simulation model has been approved through history by matching of these three wells as presented in Fig. 10. The calculated initial oil in place by the simulation model was found to be equal to 2064110111 STB. This value was compared with a corresponding one calculated by the geological model (1969497011 STB). The percentage error was found to be equal to 4.6 %. This confirmed the reliability of the simulation model. It was crucial to gain confidence in the numerical models by validating the models and results by use of laboratory results. To obtain a more accurate CO_2-compositional simulation model, the capillary pressure and relative permeability needed to be consistent with the permeability/porosity variations of the rocks (Webber and Van Geuns 1990). The published experimental results (El-Maghraby et al. 2011; Krause et al. 2009; Perrin and Benson 2010; Cai and Hicks 1999) revealed the strong dependency of the CO_2 saturation distribution on porosity and permeability heterogeneity. Giraud et al. (1971) and Henry and Metcalfe (1983) reported that the realistic permeability data must be used in evaluating the volumetric sweep-out. The migration and trapping of injected CO_2 are controlled mainly by the interplay of the capillary pressure. Capillary pressure curves and relative permeability curves consistent with the rock properties and heterogeneities should be obtained through a laboratory core analysis (Bennion and Bachu, 2006). In the current study, the permeability–porosity models were generated based on the core oil/brine experimental results[15]. The reliability of these models has been approved by comparing the results with the oil/brine experimental results. These models were utilized to generate the permeability for each well interval.

The fluid behavior in the miscible compositional simulation model depended mainly on the EOS PVT model which has been approved as discussed in the PVT model section. There were three phases considered in the model, oil, water and gas and the MISCIBLE option, which were activated. The HCSCAL option was activated to allow performing an extra scaling of the hydrocarbon relative permeabilities. Because, in the current study, the gas relative permeability of the connate water differed from the oil relative permeability, a discontinuity occurred in the hydrocarbon relative permeability as the system became two phases. The HCSCAL option scaled krg near the critical point in an analogous manner to the hydrocarbon relative permeability to avoid a discontinuity. In the current study, the considered relative permeability for the oil–water and gas–oil systems, and capillary pressure analysis were gathered from laboratory measurements. The three-phase relative permeability curves were calculated considering zero residual gas saturation and different residual water and oil saturations for the oil–water relative permeability system. For the gas–oil relative permeability system, different residual gas, oil and water saturations were considered.

Composition of the injected fluid

In the current study, pure CO_2 has injected; however, when simulating CO_2-injection with 100 % purity of CO_2, problems near-critical conditions will occur, unless the injection fluid is diluted to a certain degree. If pure CO_2 is injected, no phase envelope will be formed (Tor, 2014); instead, it will be a straight line. However, if there is a very small fraction of C_1 and N_2, the mixture will form a phase envelope and Eclipse will have a bigger margin of calculating phase properties. The phase properties should be approximately equal to that of pure CO_2 if the fractions of the impurities are very small. The injection gas

components considered in the current study are shown in Table 2. Moreover, it is important to note that in reality the CO_2-injected will always contain some impurities. Additionally, by injecting pure CO_2 it may cause the grid blocks to only contain CO_2. This causes problems for Eclipse since two or more components are needed to perform a flash calculation.

Waterflooding (WF)

The waterflooding technique has proved to be the most popular and successful secondary oil recovery mechanism. This recovery method has been used on numerous oil fields worldwide. However, after the secondary recovery process, there is still a significant amount of oil trapped in the reservoir. In the current study, the waterflooding process was tried after the natural depletion of the reservoir. There have been six producers already drilled; these producers were located almost in the middle of the formation. There were 50 infill drillings suggested as the optimum well locations (Al-Khazraji and Shuker 2015a, b). The waterflooding process was achieved through 21 injectors. These injectors were located depending on the reservoir heterogeneity and in a way that would provide enough support to the producers. The waterflooding process has been optimized to start in January 2027 as a secondary recovery method after depletion of the reservoir, naturally, for 10 years. Several waterflooding options were tried with different injection rates at each injector as follows: 1000, 1250, 1500, 2000, 2500 and 3000 STB/day. The waterflooding process has been optimized to halt in January 2056 and start the miscible CO_2-flooding process because of the incomparable oil recovery obtained for different injection rates as shown in Fig. 11. The simulator runs were conducted using the compositional simulator for the compatibility purpose in order to import the restart file data of the waterflooding case into the CO_2 compositional simulator runs. The setup for the simulation model was the following: All production wells were set on the constant production rate of 3000 STB/day, with a bottomhole pressure limit of MMP for the CO_2 injection. The production at the well stopped as the watercut level of 80 % was reached. The injection rates were adjusted to avoid the pressure increase over the formation fracture pressure.

The results are presented in Fig. 11. As it can be seen, the injection rate option of 3000 STB/day has reflected the higher reservoir production rate. The results were analyzed economically depending on the NPV calculations; these results are presented in Fig. 12. The higher NPV was also realized at the injection rate option of 3000 STB/day. This case was considered as the base of which the CO_2-miscible injection process was continued.

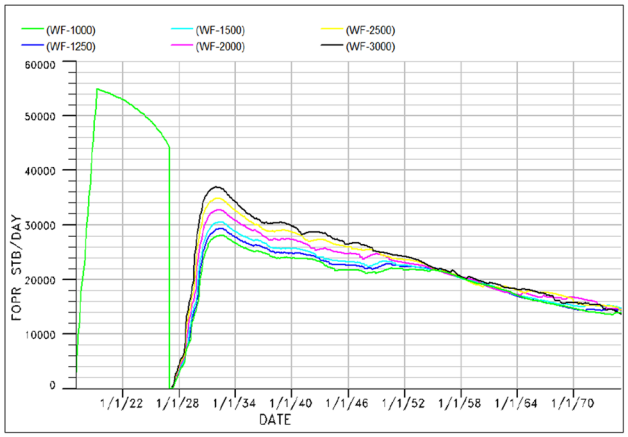

Fig. 11 Reservoir performance under different waterflood scenarios

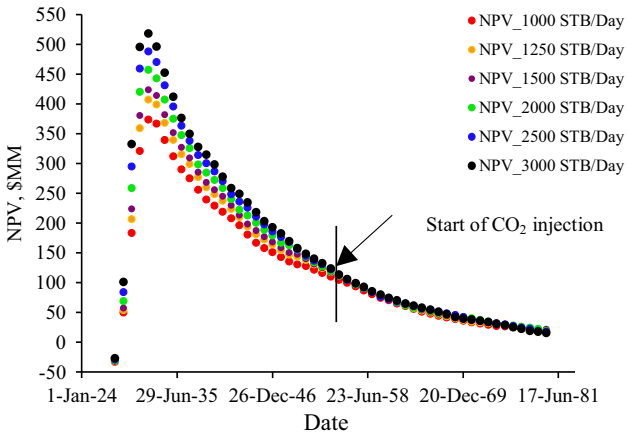

Fig. 12 NPV for different waterflood scenarios

Continuous carbon dioxide injection (CCO_2)

This technique involves injecting a certain amount of CO_2 continuously until the required slug size is reached. Usually, continuous miscible CO_2-injections have excellent microscopic displacement efficiency. But, they often suffer from poor macroscopic sweep efficiency due to the formation of viscous fingers that propagate through the CO_2 passing much of the hydrocarbon that has not been contacted. This happens as a result of the low viscosity of the CO_2 compared to the oil, and it results in an adverse mobility ratio.

In this study, the miscible carbon dioxide injection was started up after the waterflooding process had been completed. The optimum waterflooding strategy was chosen as the base to continue the CO_2-injection process. In this issue, several compositional simulation runs were conducted to optimize to the optimum the CO_2-injection rate that reflected the highest net present value. A wide range of injection rates was trying to examine the reservoir

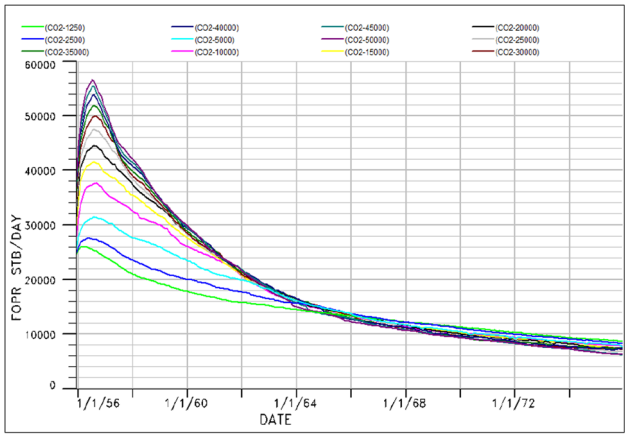

Fig. 13 Reservoir performance comparison under different CO_2-flooding scenarios

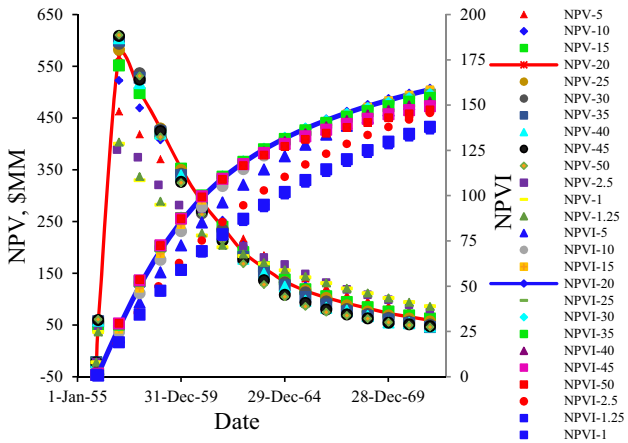

Fig. 14 NPV and NPVI for different continuous CO_2 scenarios

performance under the miscible CO_2-injection. These rates included: 5, 10, 15, 25, 40 and 50 MM Scf/day. The setup for the simulations was the following: All production wells were set at the constant production rate of 3000 STB/day, with the bottomhole pressure limit of MMP. The CO_2 was injected at a constant rate for each development strategy, with the maximum bottomhole injection pressure limit of the formation fracture pressure. The production wells were closed when the watercut reached the limit of 95 %, and the injection rates were adjusted to avoid a pressure increase over the fracture pressure. All the results were analyzed relative to the net present value calculations as the economic criterion.

The results showed that the injection rate option of 50 MScf/day has reflected the higher oil recovery for the first 6 years of the reservoir production as shown in Fig. 13. But economically, the injection rate option of 20 MScf/day has reflected the higher NPVI as shown in Fig. 14. This injection rate was considered as an optimal CO_2-injection rate for all the CO_2-flooding modes.

Table 6 Water injection rate for different WAG ratio

NO	CO_2-WAG	Qw_{inj} STB/day
1	1:1	9643
2	1.5:1	14465
3	1:1.5	6432
4	1:2	4822
5	1:2.5	3857
6	1:3	3211
7	1:3.5	2758
8	1:4	2411

Water-alternating-CO_2-injection (CO_2-WAG)

The CO_2-WAG technique is a combination of two traditionally improved oil recovery techniques: waterflooding and gas injection. The waterflooding and gas flooding cycle lengths are alternated with the design parameters being the cycle timing of the WAG process and the ratio of water to gas, slug size of the injected CO_2 and water. The main advantage of this technique is to reduce the CO_2 channeling by filling the highly permeable channels with water to improve the macroscopic sweep efficiency during the CO_2-injection. The optimum conditions of the oil displacement by the WAG processes are achieved when the velocities of the gas and water are the same in the reservoir and hence stabilize the sweeping front. The optimum WAG design varies from reservoir to reservoir depending on the reservoir heterogeneity and characteristic. The main advantages of the WAG process include reduced CO_2 utilization and production, and greater ultimate recovery.

In the current study, the CO_2-WAG injection process proceeded after the waterflooding process has completed. Under this strategy, several compositional simulation runs were modeled to optimize the CO_2-WAG process for the Nahr Umr reservoir. The setup for the simulations was the following: All production wells were set at the constant production rate of 3000 STB/day, with the bottomhole pressure limit of MMP. The production wells were closed when the watercut reached the limit of 95 %, and the injection rates were adjusted to avoid a pressure increase over the fracture pressure.

Two cases were considered here; the first one included utilizing the economically optimum CO_2-injection rate determined in the CCO_2-injection process of 20 MM Scf/day. Eight cases with different CO_2-WAG ratios were

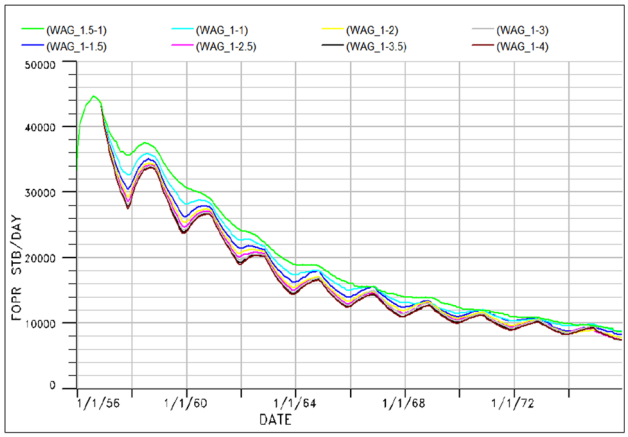

Fig. 15 Reservoir performance comparison under different CO_2-WAG ratio flooding scenarios

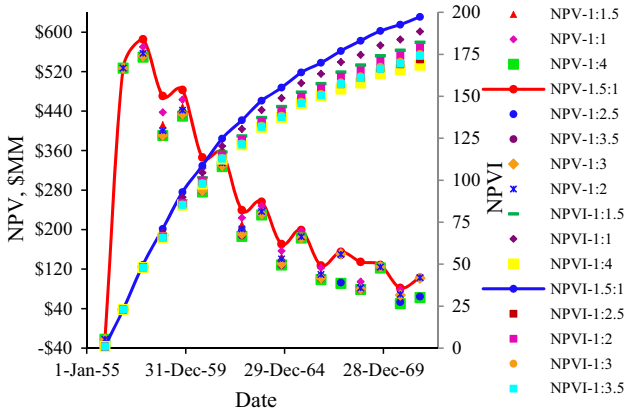

Fig. 16 NPV and NPVI for different CO_2-WAG ratio scenarios

simulated and evaluated. They were 1:1, 1:1.5, 1:2, 1:2.5, 1:3, 1:3.5, 1:4, 1.5:1 and 2:1. The corresponding water injection rate for each CO_2-WAG ratio was determined by utilizing Eq. (11) as the CO_2-injection rate remained constant as shown in Table 6. The cycle lengths for each phase of all eight trials were set for a year. The results showed that the CO_2-WAG process option of a 1.5:1 CO_2-WAG ratio has reflected the higher oil recovery and NPVI at the same time as shown in Figs. 15 and 16.

The second case included utilizing the optimum CO_2-WAG ratio to investigate the optimum CO_2-WAG injection for varying the cycle time. Eight trials were considered, including 3, 6, 9, 12, 18, 24, 30 and 36 months half-cycle lengths for each phase. All the results were analyzed relative to the net present value calculations. The results showed that the CO_2-WAG injection with a 1.5:1 CO_2-WAG ratio and 12 months half-cycle lengths has reflected

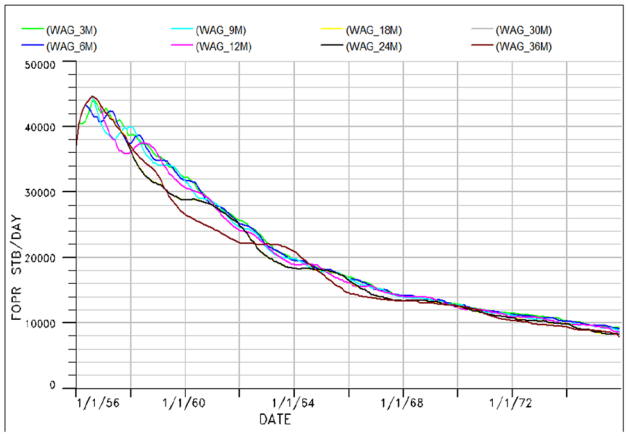

Fig. 17 Reservoir performance comparison under different CO_2-WAG cycle length scenarios

the higher oil recovery and NPVI at the same time as shown in Figs. 17 and 18.

$$Q_w = \frac{Q_{CO_2} \times B_{CO_2} \times \mathrm{WACO_{2ratio}}}{B_w} \quad (11)$$

Hybrid-CO_2-WAG injection

This technique is achieved when a large slug of CO_2 was injected followed by a number of small slugs of water and CO_2. In the current study, this technique has been achieved by utilizing the optimum CO_2-WAG injection mode portion and the optimum injection rate for the initial CO_2-injection rate. The effects of varying the initial CO_2 slug size on the recovery factor for the hybrid CO_2-WAG were studied. The setup for the simulations was the following: All production wells were set at a constant production rate of 3000 STB/day, with the minimum bottomhole pressure of MMP. The production wells were closed when the watercut reached the limit of 95 %, and the injection rates for the water and CO_2 were adjusted to avoid a pressure increase over the formation fracture pressure.

Five trials with varying initial CO_2 slugs, including 10, 20, 30, 40, and 50 % HCPV, were modeled. The initial CO_2 slug size was defined by prolonging the cycle time of the initial CO_2-injection until the required initial CO_2 slug size was met. The required slug size in terms of HCPV is presented in Table 7. The results are presented in Figs. 19 and 20. It was shown that the mode of the initial CO_2 slug size of 10 % injection reflected the higher NPVI and oil production.

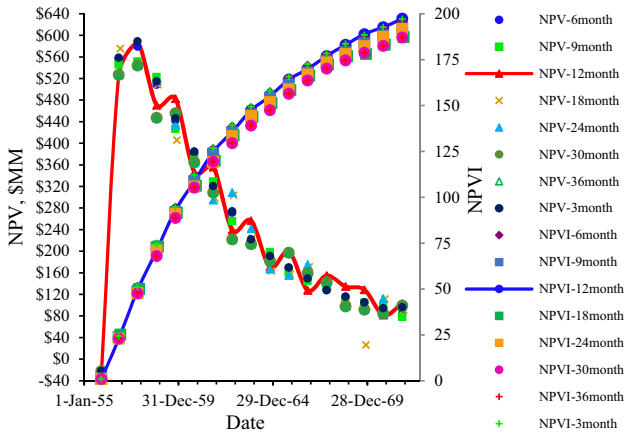

Fig. 18 NPV and NPVI for different CO_2-WAG cycle length scenarios

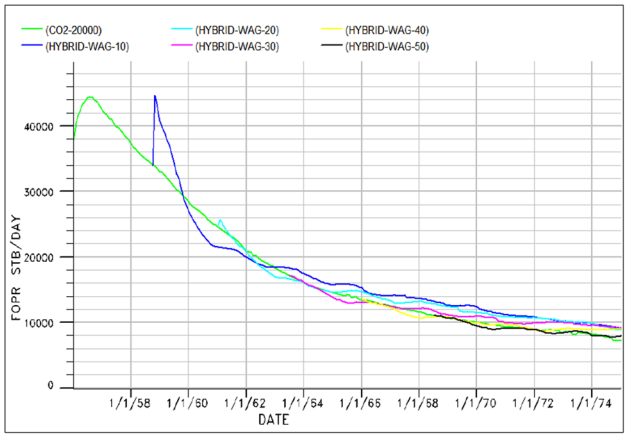

Fig. 19 Reservoir performance comparison under different Hybrid CO_2-WAG injection scenarios

Table 7 Hydrocarbon pore volume required for hybrid WAG process

No	CO_2 slug Size %	HCPV rbbl	Period day
1	10	187855561.6	913
2	20	375711123.2	1826
3	30	563566684.8	2739
4	40	751422246.4	3652
5	50	939277808.0	4565
6	60	1127133370	5479
7	70	1314988931	6392
8	80	1502844493	7305
9	90	1690700054	8218
10	100	1878555616	9131

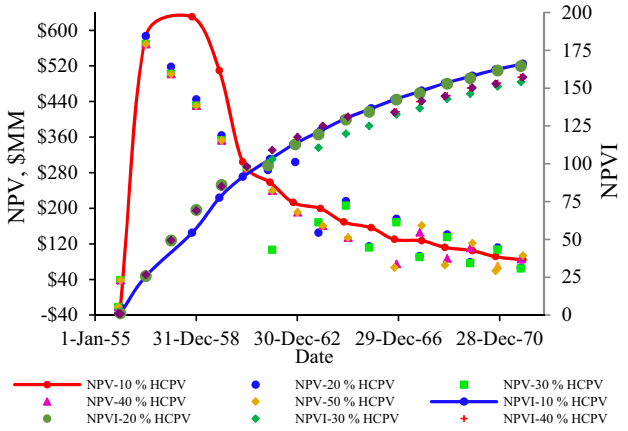

Fig. 20 NPV and NPVI for different Hybrid CO_2-WAG scenarios

Simultaneous water and CO_2-injection (CO_2-SWAG)

This technique involves injecting water and CO_2 in combination into the reservoir at the same well. The mixing of CO_2 and water in a CO_2-SWAG injection can be at the downhole or on the surface. Surface mixing usually occurs at the well, drill site or at the central processing facility. The objective of this technique is to improve the sweep efficiency of the CO_2-flooding by reducing the impact of viscous fingering. At the same time, this reduces the capital and operating costs and finally will result in an improvement in gas handling and oil recovery (Ma et al. 1995; Sanchez 1999). The simultaneous water and gas injection can be difficult to implement and there can be some practical difficulties associated with this technology.

In this study, the CO_2-SWAG process was tested through five modeled compositional simulation runs to analyze the effects of different CO_2-injection rates for the CO_2-SWAG injection on the recovery factor. The setup for the simulations was the following: All production wells were set at a constant production rate of 3000 STB/day, with the minimum bottomhole pressure of MMP. The production wells were closed when the watercut reached the limit of 95 %, and the injection rates for the water and CO_2 were adjusted to avoid a pressure increase over the formation fracture pressure. To determine the optimum CO_2-SWAG injection rate, the CO_2-SWAG ratio was fixed at 1:1 and the accompanying water injection rates were determined using Eq. (11). The CO_2-injection rates considered for this case were: 5000, 7500, 10000, 12500 and 15000 MScf/day. The accompanying water injection rates were calculated using Eq. (11) as shown in Table 8.

The results have been presented in Figs. 21 and 22. It can be seen that the CO_2-SWAG process option of 15000 MScf/day CO_2-injection and 7232 STB/day water injection has reflected the higher oil recovery and NPVI at the same time.

Table 8 Water injection rate for different SWAG process

NO	$WACO_2$	QCO_2 MScf/day	Qw_{inj} STB/day
1	1:1	5000	9643
2	1:1	7500	14465
3	1:1	10000	6432
4	1:1	12500	4822
5	1:1	15000	3857

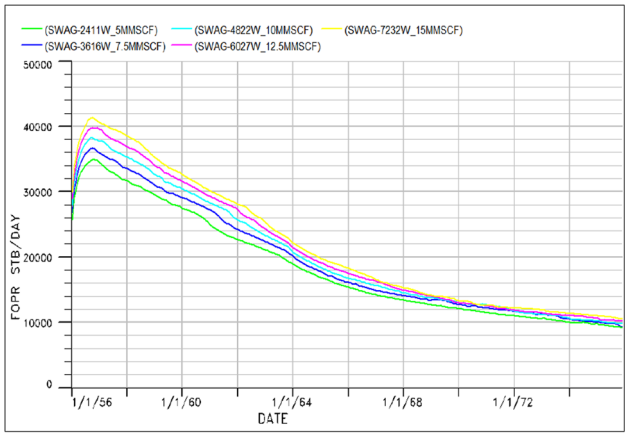

Fig. 21 Reservoir performance comparison under different CO_2-SWAG scenarios

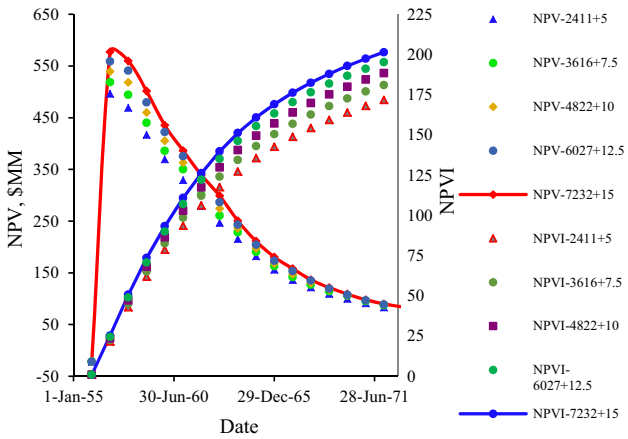

Fig. 22 NPV and NPVI for different CO_2-SWAG scenarios

In order to determine the optimum CO_2-SWAG ratio on the recovery factor, five CO_2-SWAG ratios were simulated and evaluated. They were 1:1, 1:2, 1:3, 1.5:1 and 2:1. The optimum CO_2-$SWACO_2$ injection rate calculated from the previous step (15000 MScf/day) was used as a constant. But, the accompanying water injection rate was varied for all of the five cases according to their water to the CO_2-$SWACO_2$ ratio. The required water injection rates to make up the CO_2-SWAG ratio were calculated using Eq. (11) as shown in Table 9.

Table 9 Water injection rate for different SWAG ratio

NO	$WACO_2$	QCO_2 MScf/day	Qw_{inj} STB/day
1	1:1	15000	7232
2	1:2	15000	3616
3	1:3	15000	2408
4	1.5:1	15000	10849
5	2:1	15000	14465

The results are presented in Figs. 23 and 24. It can be seen that the CO_2-SWAG process option of a 2:1 CO_2-SWAG ratio has reflected the higher NPVI and oil recovery at the same time.

Results and discussion

Heterogeneous reservoirs are known to have a low recovery factor due to pressure development within the reservoir, multiphase phase behavior, reservoir compartmentalization, capillary pressure and viscosity effect (Bennion and Bachu, 2006). The results reflected a successful CO2-flooding process in all modes because the obtained recovery factors were in the expected range. However, many wells were closed during the prediction period due to reaching the watercut's the maximum limit and causing a reduction in the oil recovery. For CCO_2-flooding modes, it was observed that by increasing the CO_2-injection rate, an increase in the field oil production rate (FOPR) at an earlier stage was achieved. However, the ultimate FOPR stayed in approximately the narrow range after 8 years of the predicted period. This was due to the development of a gas channel between the injectors and producers. From Figs. 25, 26 and 27, it can be seen that by implementing the CCO_2-flooding with the lower injection rate set to 5 MMScf/day, the injected amount of CO_2 was not enough to achieve efficient displacement. The injection rate of 20 MMScf/day reflected a consistent, efficient oil sweeping as the distribution of the injected CO_2 was almost uniform in the reservoir. Therefore, the stabilized displacement gave an upward shift in the NPV and NPVI curves, Fig. 14. In the case of a high CO_2-injection rate with a 50 MMScf/day, the CO_2-injected distribution exhibited higher CO_2 saturation in the reservoir, especially in the parts of high connectivity (indicated by the red color). This led to developing gas channels in the reservoir, especially in the part of high connectivity. In this case, the channeling of gas was more prominent and a lot of gas was back produced. This explained getting a high produced GOR during the predicted period. As more CO_2 was produced as the unstable displacement front and more separation and recycling cost was required, hence, there was a reduction in the project profitability.

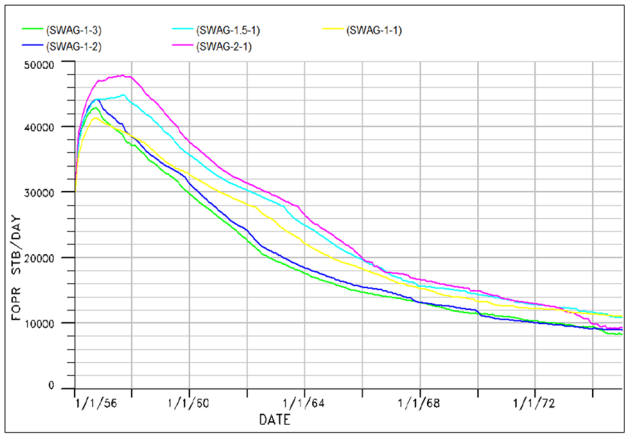

Fig. 23 Reservoir performance comparison under different CO_2-SWAG ratio scenarios

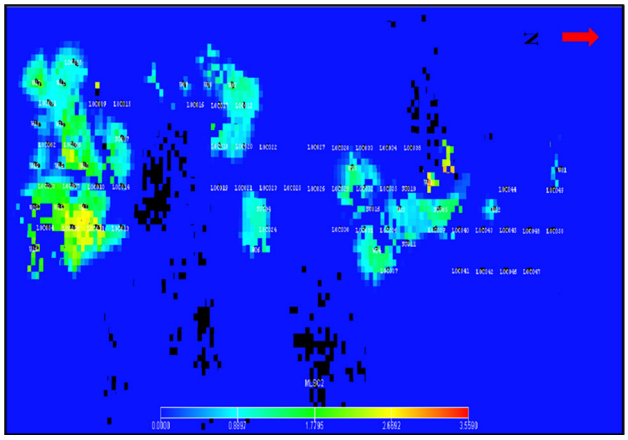

Fig. 25 CO_2-distibution for CO_2-injection rate set to 5000 MScf/day at Jan/2072

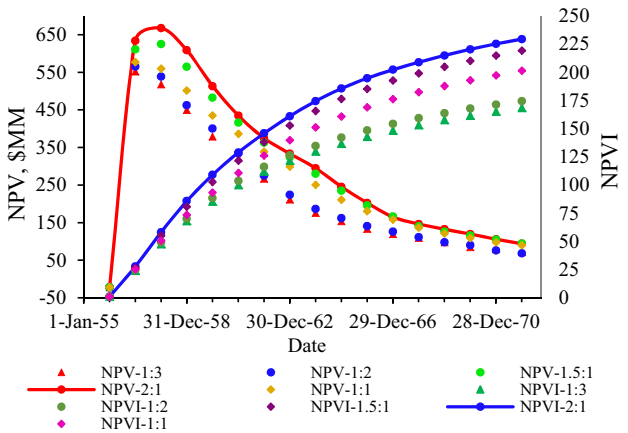

Fig. 24 NPV and NPVI for different CO_2-SWAG ratio scenarios

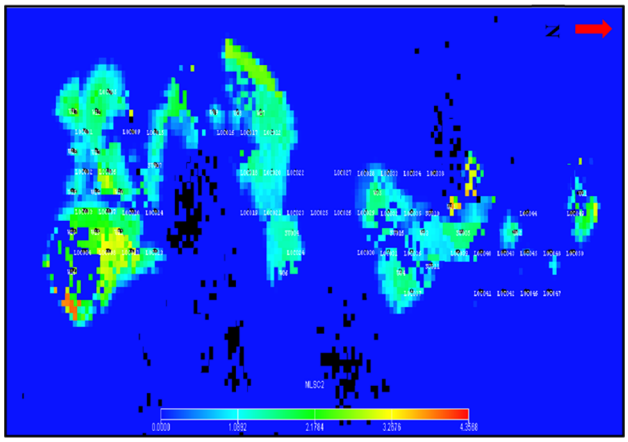

Fig. 26 CO_2-distibution for CO_2-injection rate set to 20000 MScf/day at Jan/2072

For the WAG injection scheme, the CO_2-WAG flooding with a low WAG ratio of 1:4 reflected the less oil recovery and profitability. This reflected that lower mobility control of CO_2 had been occurring and then bypassed a large amount of oil. As the WAG ratio increased to a certain extent, the oil recovery and economic feasibility improved. This reflected the improvement in gas mobility control through increasing the amount of injected water. Moreover, the low WAG ratio caused early gas breakthrough and gas channeling; hence, oil was trapped and not allowed sufficient gas–oil contact. The WAG ratio of 1.5:1 reflected the highest oil recovery and economic feasibility. From Figs. 28, 29 and 30, it can be seen that the CO_2 saturation distribution for the second case was higher and consistent which means that there were stable microscopic displacement and mobility control for CO_2. At the same time, the macroscopic displacement was better managed in this case. This amount of water was sufficient to realize the mobility control and stable displacement front. The one-year half cyclic length reflected the highest oil recovery and economic feasibility, although the CO_2 saturation distribution did not exhibit an appreciable difference for different cyclic lengths. The economic analysis shows an outperformance of a 1-year half cycle over the others. However, the 1-year half cyclic length is considered more convenient, practically, to apply than the shorter cycles. This process was tried till a 31.6 % HCPV CO_2 slug size had been injected for the date January 2072. If the process continues longer, the expected oil recovery increment will be higher. The simulation time was limited to January 2072 due to the length of time it would take and large computational cost if the predicted time was extended. It is worth noticing that it was difficult to differentiate between different CO_2-WAG injection processes based on oil recovery alone without combining the results with the economic analysis. Figures 31, 32 and 33 show the CO_2 saturation distribution for this case.

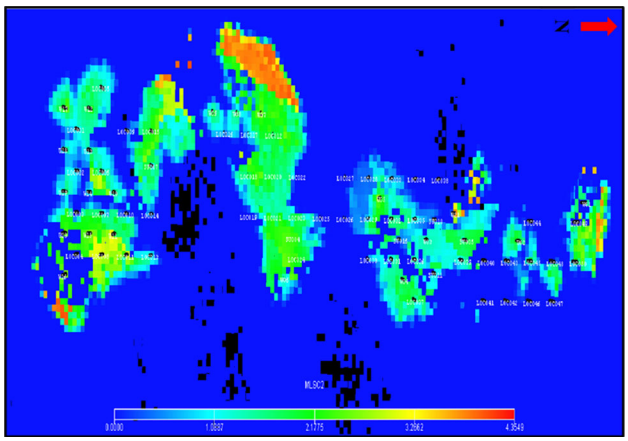

Fig. 27 CO_2-distibution for CO_2-injection rate set to 50000 MScf/day at Jan/2072

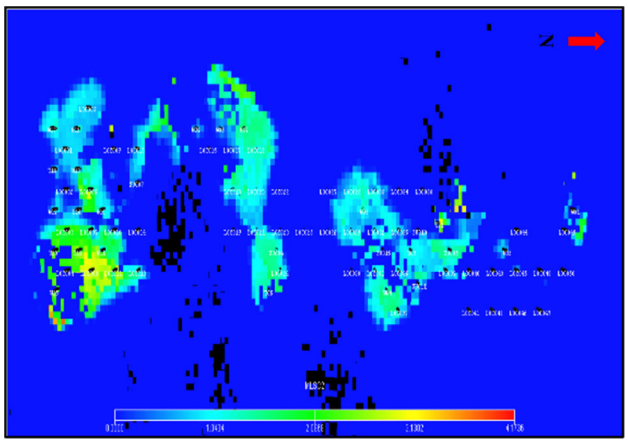

Fig. 29 CO_2-distibution for WAG ratio set to 1–2 at Jan/2072

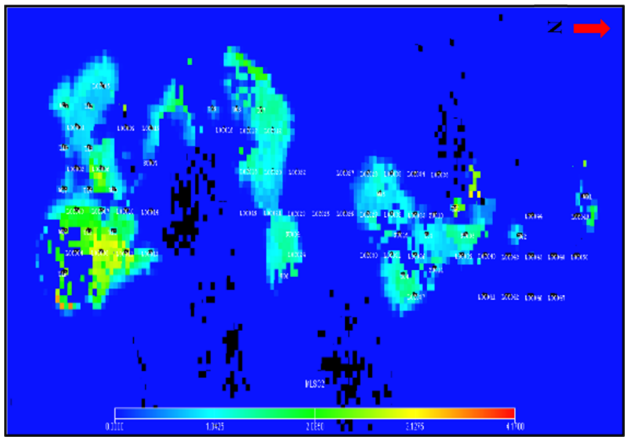

Fig. 28 CO_2-distibution for WAG ratio set to 1–4 at Jan/2072

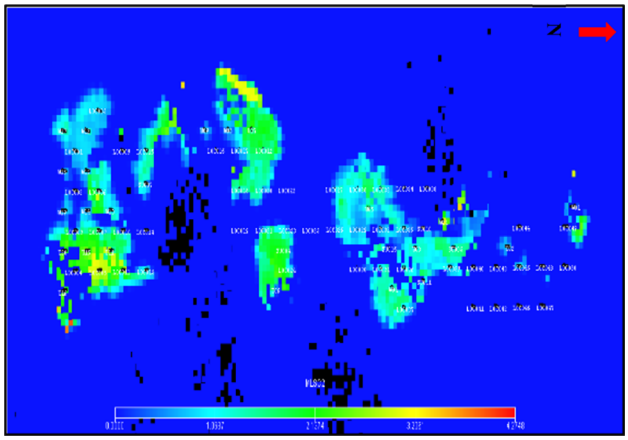

Fig. 30 CO_2-distibution for WAG ratio set to 1.5–1 at Jan/2072

In the CO_2-SWAG process, it has been concluded that the gas efficiency factor (incremental oil produced per volume of gas injected) decreases with larger gas injection volumes. The optimum amount of the injected gas has to be used. From Figs. 34, 35, 36 and 37, it can be seen that the saturation of CO_2 was less compared to the other CO_2-injections modes, as the required amount of injected CO_2 was also less. Accordingly, the reduced injected slug size led to reduced project cost, hence increased profitability for the SWAG process. In conclusion, the injection water, in alternating slugs or simultaneously with gas forms, yields a more stable displacement front, hence better project profitability over other CO_2-injection modes. The water phase acts for more mobility control of gas, hence better microscopic displacement.

In the case of the hybrid CO_2-WAG injection, the one of a 10 % initial CO_2 slug size injection reflected a higher NPV and oil production among the other hybrid WAG modes. With the greater CO_2 slug size injection, the more inconsistent the sweep efficiency was, due to the unfavorable mobility of the CO_2 and the reservoir heterogeneity. The incremental oil recovery for the hybrid process was less than that for the CCO_2 process; but, the economic profitability of the hybrid process was better due to the large cost of the required injected CO_2 in the case of the CCO_2 process. As compared to the WAG process, the incremental oil recovery for the hybrid process was 0.189 % less. The gas injection alone often resulted in poor sweep efficiency due to the early breakthrough caused by the unfavorable gas–oil mobility ratio. This explained the outperformance of the hybrid process of the 10 % HCPV injection slug over the others as the large solvent slug sizes, per WAG cycle, caused channeling and increased cost, substantially. The minimizing of the slug size, per WAG cycle, maximized the profitability of the solvent floods. The solvent contacted more oil, and channeling was minimized when the CO_2 slug size, per WAG cycle, was decreased. However, the achieved oil recovery by the

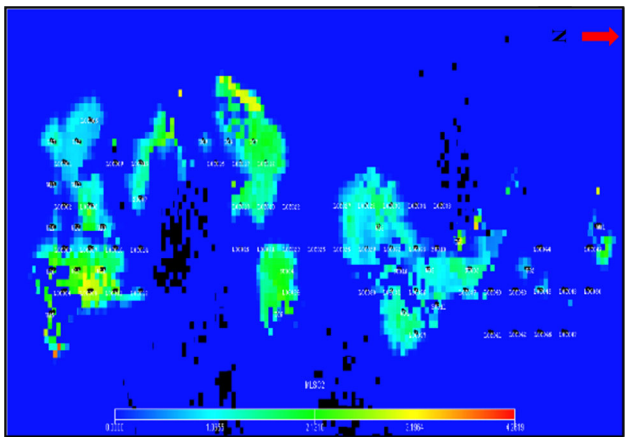

Fig. 31 CO_2-distibution for WAG cyclic length set to 6 month at Jan/2072

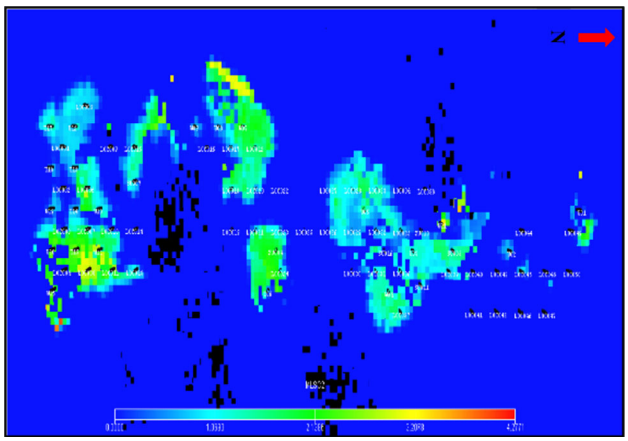

Fig. 32 CO_2-distibution for WAG cyclic length set to 12-month at Jan/2072

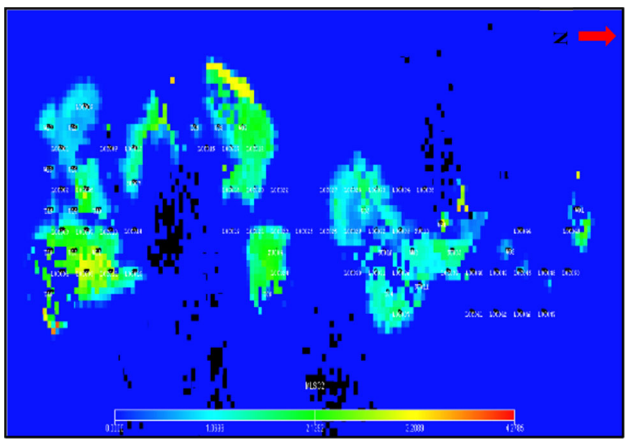

Fig. 33 CO_2-distibution for WAG cyclic length set to 24-month at Jan/2072

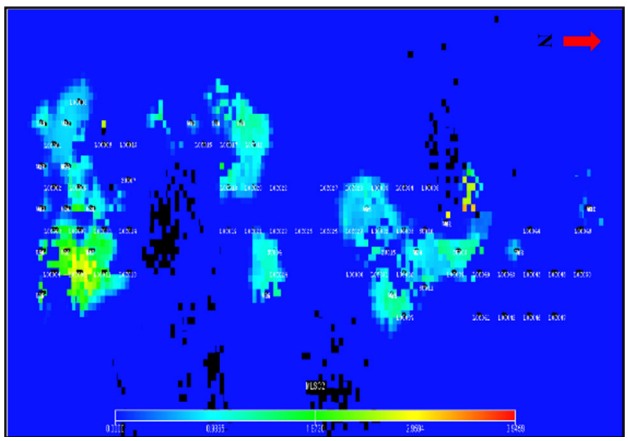

Fig. 34 CO_2-distibution for CO_2-SWAG rate set to 2411 bbl/day (water) and 5 MMScf/day (CO_2) at Jan/2072

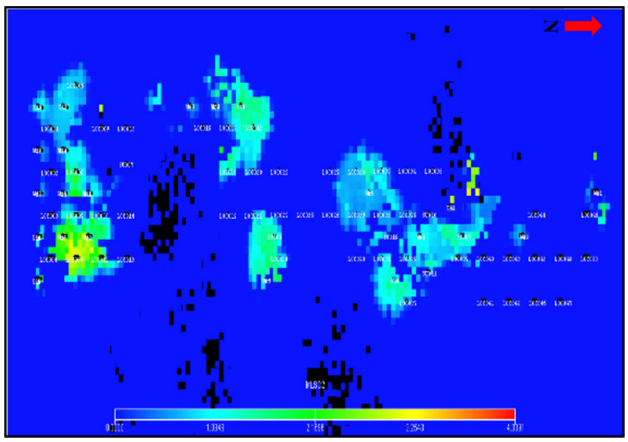

Fig. 35 CO_2-distibution for CO2-SWAG rate set to 6072 bbl/day (water) and 12.5 MMScf/day (CO2) at Jan/2072

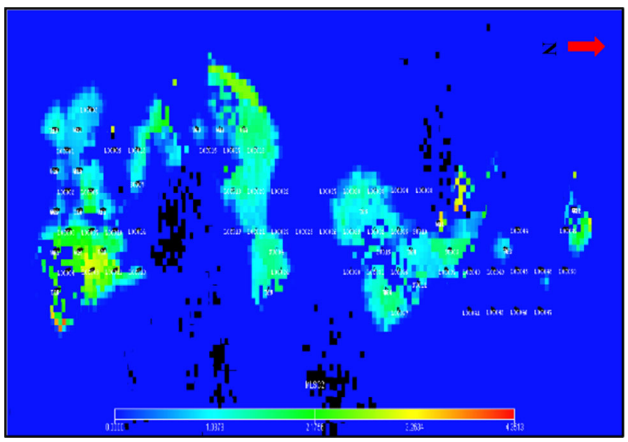

Fig. 36 CO_2-distibution for SWAG ratio set to 1–3 at Jan/2072

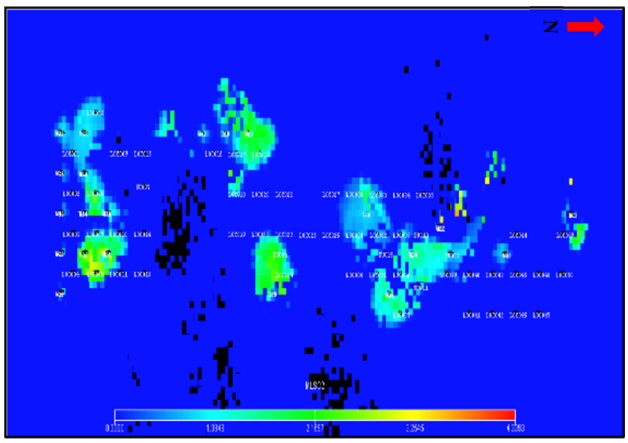

Fig. 37 CO_2-distibution for SWAG ratio set to 2–1 at Jan/2072

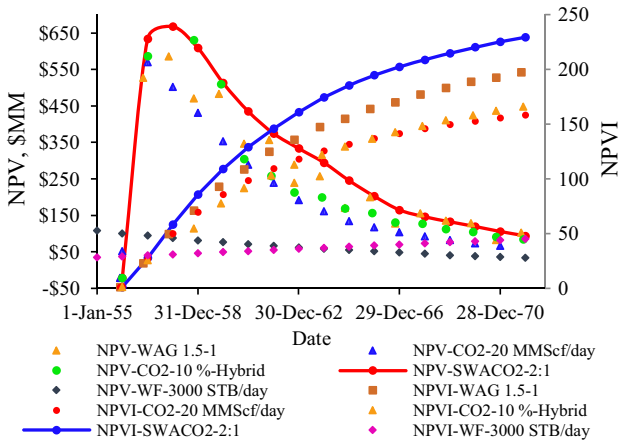

Fig. 38 NPV for different CO_2-flooding modes and waterflooding scenarios

WAG and SWAG processes was higher than the corresponding one of the CCO_2-flooding processes. This confirmed the improvement in the sweep efficiency by stabilizing the displacement front, and in particular, it was helpful in severe heterogeneity, gravity overrides and reduction in the capillary entrapment of the oil.

In this study, it was observed that the vast majority of producers became wet very soon and the water production increased for most of them. This required the use of an artificial lift method to keep the wells production and enhance oil recovery. However, the objective here has been to investigate the contribution of the CO_2-injection modes individually to improve oil recovery. In conclusion, the CO_2-SWAG mode of the 2:1 SWAG ratio has reflected the higher NPVI over other CO_2-injection modes. The incremental oil recovery from the CO_2-SWAG process was 9.174 % higher than the waterflooding case, 1.113 % in comparison with the CCO_2-flooding case, 1.176 % in comparison with the hybrid CO_2-WAG case and almost 0.987 % when compared with the CO_2-WAG case. The results have been shown in Fig. 38 and Table 10.

Observations and conclusions

The observations and conclusions drawn from this study are summed up below:

1. This study is enough to give answers to what will be the performance of Nahr Umr reservoir and other clastic heterogeneous reservoirs in the southern of Iraq under miscible CO_2-flooding processes.
2. The MMP calculated by the Glaso (1985) method was considered in the current work because the average molecular weights of the fluid samples utilized in preparing the Glaso correlation were almost near the molecular weight of the Nahr Umr reservoir fluid. Moreover, it gave an average value among the other correlations.
3. The CCO_2 has resulted in the poorest economic profitability in front of the other CO_2-injection modes, whereas WAG and SAWG processes have resulted in better performance.
4. As the reservoir heterogeneity increases, there is a need to apply WAG and SWAG process implementation to increase oil recovery.
5. It is necessary to conduct a detailed economic analysis to prove the most effective process among different CO_2-injection modes.
6. The CO_2-injections modes have fulfilled expectations.

Table 10 NPVI for different development options

Injection mode	Producers	Injectors	Period years	Gas Inje. rate (MMScf/Day)	Water Inje. rate (STB/Day)	WC (%)	Cum. oil MMSTB	FOE (%)	NPVI
WF	56	21	28	0	3000	51.89	451.19642	22.524	59.0057
CCO_2	56	21	16	20	0	83.39	569.8769	30.585	158.4938
CO_2-WAG	56	21	16	20	3000	83.08	582.5244	30.711	197.3218
Hybrid-CO_2-WAG	56	21	16	20	3000	83.93	575.3267	30.522	166.0301
SWG-Diff-CO_2-rate	56	21	16	20	3000	83.61	590.9341	30.703	201.4182
SWG-Diff-SWAG ratio	56	21	16	20	3000	86.70	611.5333	31.698	229.4477

7. The SWAG injection process proved as a means to provide better mobility control of gas than the WAG injection.
8. The oil production rate for all CO_2-flooding scenarios showed the typical behavior with the increase in the oil production at the beginning of injection period and then a drop because the production wells were closed, due to reaching the watercut limit. Therefore, it requires application the artificial lift means to enhance oil recovery.

Acknowledgments Our thanks mainly go to the Iraqi Ministry of Oil for permission to publish this paper and to the PETRONAS Oil Company that has supported this work.

References

Ahmed T (2005) Advanced reservoir engineering. Gulf Professional Publishing Company, USA

Ahmed T (2010) The practice of reservoir engineering (Revised Edition). Gulf Professional Publishing Company, USA

Al-Khatteeb LJ (2013) Natural gas in the Republic of Iraq. 2013, James A. Baker III Institute for Public Policy, Rice University

Al-Khazraji AK, Shuker MT (2014a) Multiple liner regression approach for the permeability calculation from well logs: a case study in Nahr Umr formation-Subba oil field. Int J Sci Res (IJSR) 3(6):1408–1415

Al-Khazraji AK, Shuker MT (2014b) Integrated petrophysical evaluation of a heterogeneous shaly-sand reservoir: a case study in Nahr Umr Formation-Subba giant oil field, Iraq. Res J Appl Sci Eng Technol 49(10):75–82

Al-Khazraji AK, Shuker MT (2015a) Development of heterogeneous immature brownfield with water drive using dynamic opportunity index: a case study from Iraqi oil fields. Presented at the North Africa technical conference and exhibition, Cairo, Egypt, SPE-175708-MS

Al-Khazraji AK, Shuker MT (2015b) Optimal field development of immature clastic heterogeneous brownfield: Suba field, South Iraq case study. Presented at the North Africa technical conference and exhibition, Cairo, Egypt, SPE-175740-MS

Al-Mudhafar WJ (2013) A practical economic optimization approach with reservoir flow simulation for infill drilling in a mature oil field. Presented at the North Africa technical conference and exhibition, Cairo, Egypt, SPE 164612

Alston RB, Kokolis GP, James CF (1985) CO_2 minimum miscibility pressure: a correlation for impure CO_2 streams and live oil systems. Soc Petrol Eng J 25(2):268–274

Aqrawi AM, Jeremy CG, Horbury AD, Sadooni FN (2010) The petroleum geology of Iraq. Scientific Press Ltd, UK

Babadagli T (2005) Mature field development—a review. Presented at the SPE Europec/EAGE annual conference, Madrid, SPE 93884

Bailey B, Crabtree M, Tyrie J, Elphick J, Kuchuk F, Romano C, Roodhart L (2000) Water control. Oilfield Rev, 12(1):30–51

Behrouz R, Ghazanfari MH (2004) Critical design factors and evaluation of recovery performance of miscible displacement and WAG process. Presented at the 55th annual technical meeting, Calgary, Alberta, Canada

Bennion DB, Bachu S (2006) The impact of interfacial tension and pore size distribution/capillary pressure character on CO_2 relative permeability at reservoir conditions in CO_2-brine system. In: SPE/DOE symposium on improved oil recovery. Society of Petroleum Engineers, Tulsa, p 10

Broome JH, Bohannon JM, Stewart WC (1986) The 1984 Natl. Petroleum Council Study on EOR:An Overview. J Petrol Technol 38(8):869–874

Cai Z, Hicks PJ Jr (1999) 3D conditional simulation of porosity for a heterogeneous core. J Can Pet Technol 38(1):46–52

Capillary Pressure Experiments by Pressure Decreasing Technical Report for Well Su-12 in Nahr Umr Reservoir-Subba Oilfield (1978) Ministry of Oil, Baghdad, Iraq, unpublished report

Chen S, Li H, Yang D (2009) Production optimization and uncertainty in a CO_2 flooding reservoir. Presented at the SPE production and operations symposium, Oklahoma City, Oklahoma, USA, SPE 120642

Christensen JR, Stenby EH, Skauge A (1998) Review of WAG field experience. Presented at the international petroleum conference and exhibition, Villahermose, Mexico, SPE 39883

Core Measurements Reports for Nahr Umr Formation-Subba Oilfield (1976–1980) Ministry of Oil, Baghdad, Iraq, unpublished report

Corey AT (1954) The interrelation between gas and oil relative permeabilities. Producers monthly 19(1):38–41

Cronquist C (1978) Carbon dioxide dynamic miscibility with light reservoir oils. In Proc. Fourth Annual US DOE Symposium, vol 1, Tulsa, pp 28–30

Eclipse Simulation Software Manual (2013) Schlumberger corporation, version 2013.1

El-Maghraby RM, Penland CH, Blunt MJ (2011) Coreflood measurements of CO_2 trapping. Presented at the SPE annual technical conference and exhibition, Denver, Colorado, USA, SPE 147373

Final Geological Reports for Nahr Umr Formation-Subba Oilfield (1976–1990) Ministry of Oil, Baghdad, Iraq, (1990), unpublished report

Final Well Reports for Nahr Umr Formation-Subba Oilfield (1976–1990) Ministry of Oil, Baghdad, Iraq, (1990), unpublished report

Ganesh CT, Satter A (1994) Integrated petroleum reservoir management: a team approach. PennWell Books Publishing Company, Tulsa

Geological Study for Subba Oilfield. Reservoir & Field Development Directorate, Ministry of Oil, Baghdad, Iraq, (2001), unpublished report

Ghomian Y (2008) Reservoir simulation studies for coupled CO_2 sequestration and enhanced oil recovery. Ph.D. Dissertation, Texas at Austin University, Texas

Giraud A, Thomere R, Gard J, Charles M (1971) A laboratory investigation confirms the relative inefficiency of true miscible drives, and outlines new concepts for maximizing oil recovery by gas injection. Soc Pet Eng AIME, SPE 3486

Glaso O (1985) Generalized minimum miscibility pressure correlation. Soc Pet Eng J 25(6):927–934

Hadlow RE (2004) Update of industry experience with CO_2 injection. Presented at the 67th SPE annual technical conference and exhibition, Washington, DC, Texas, USA, SPE 24928

Hao Y, Wu Z, Ju B, Chen Y (2004) Laboratory investigation of the CO_2 floods. Presented at the SPE annual technical conference and exhibition, Abuja, Nigeria, SPE 88883

Henry RL, Metcalfe RS (1983) Multiple-phase generation during carbon dioxide flooding. Soc Petrol Eng J 23(4):595–601

Jeschke PA, Schoeling L, Hemmings J (2000) CO_2 flood potential of California oil reservoirs and possible CO_2 sources. In: SPE Annual Technical Conference and Exhibition. Society of Petroleum Engineers, Dallas, p 6

Krause M, Perrin J-C, Benson SM (2009) Modeling permeability distributions in a sandstone core for history matching coreflood experiments. Soc Petrol Eng J SPE 126340

Kulkarni MM, Rao DN (2004) Experimental investigation of various methods of tertiary gas injection. Presented at the SPE annual technical conference and exhibition, Houston, Texas, USA, SPE 90589

Kulkarni MM, Rao DN (2005) Experimental investigation of miscible secondary gas injection. Paper presented at the SPE annual technical conference and exhibition, Dallas, Texas, USA, SPE 95975

Leverett M (1941) Capillary behavior in porous solids. Trans AIME, 142(1):152–169

Lohrenz J, Bray BG, Clark CR (1964) Calculating viscosities of reservoir fluids from their compositions. Presented at the annual fall meeting, Houston, Texas, SPE 915

Ma TD, Rugen JA, Stoisits RF, Youngren GK (1995) Simultaneous water and gas injection pilot at the kuparuk river field. Reservoir Impact SPE 30726

Mahnaz K, Farouq A (1984) Role of immobile phase saturation in tertiary oil recovery. Presented at the SPE/DOE fourth symposium on EOR, Tulsa, Oklahoma, USA, SPE 12635

Marylena GQ (2005) Optimization of A CO_2 flood design wasson field West Texas. M.Sc. Thesis, Texas A&M University, Texas

Mohamed E, Abdulrazag Y, Reyadh A, Hazim A (2012) Optimization of CO_2 WAG processes in a selected carbonate reservoir-an experimental approach. Presented at the SPE international petroleum exhibition and conference, Abu Dhabi, UAE, SPE 161782

Nwaozo J (2006) Dynamic of a water flood reservoir. Ph.D. Dissertation, Oklahoma University, Oklahoma

Perrin JC, Benson S (2010) An experimental study on the influence of sub-core shale heterogeneities on CO_2 distribution reservoir rocks. Transp Porous Media 82:93–109

Petrel Seismic-to-Simulation Software Manual, Schlumberger Corporation, Version (2013)

PVT Experiments report for Nahr Umr Formation-Subba Oil Field, Ministry of Oil, Baghdad, Iraq (1978) unpublished report

Rao DN, Ayirala SC, Kulkarni MM, Sharma AP (2004) Development of gas assisted gravity drainage (GAGD) process for improved light oil recovery. Presented at the SPE/DOE fourteenth symposium on improved oil recovery, Tulsa, Oklahoma, USA, SPE 89357

Reid D, David S (1997) State of the industry in CO_2 floods. Paper SPE presented at the SPE annual technical conference and exhibition, San Antonio, Texas, USA, SPE 38849

Sanchez NL (1999) Management of water alternating gas (WAG) injection projects. SPE 53714

Shyeh-Yung J-GJ (1991) Mechanisms of miscible oil recovery: effects of pressure on miscible and near-miscible displacements of oil by carbon dioxide. Presented at the 66th SPE annual technical conference and exhibition, Dallas, Texas, USA, SPE 22651

Technical Report of Capillary Pressure Experiments by Pressure Decreasing for Well Su-12 in Nahr Umr Formation-Subba Oilfield (1980) Ministry of Oil, Baghdad, Iraq, unpublished report

Technical Reports for Water Flooding Displacement Experiments for Well Su-4, 5, 7, 8, and 9 in Nahr Umr Formation-Subba Oilfield (1980) Ministry of Oil, Baghdad, Iraq, unpublished report

Thomas B, Leiv W (2002) Deep draft floater motions—verification study. Presented at the SPE offshore technology conference, Houston, Texas, USA, SPE 14303

Tor AM (2014) Optimization CO_2-injection by compositional simulation, M.Sc. Thesis, Norwegian University of Science and Technology

Webber KJ, Van Geuns LC (1990) Framework for constructing clastic reservoir simulation models. J Petrol Technol 42(10):1–248

Well Logs for Nahr Umr Formation-Subba Oilfield (1973–1980) South Oil Company, Basra, Iraq (1980) unpublished report

Yellig WF, Metcalfe RS (1980) Determination and prediction of CO_2 minimum miscibility pressures. J Petrol Technol 32(01):160–168

Yuan H, Johns RT (2004) Improved MMP correlations for CO_2 floods using analytical gas flooding theory. Presented at the SPE/DOE fourteenth symposium on improved oil recovery, Tulsa, Oklahoma, USA, SPE 89359